

The Proline-rich N-terminal Domain of G18 Exhibits a Novel G Protein Regulatory Function*

Received for publication, August 18, 2009, and in revised form, January 8, 2010. Published, JBC Papers in Press, January 22, 2010, DOI 10.1074/jbc.M109.057174

Peishen Zhao, Chau H. Nguyen, and Peter Chidiac¹

From the Department of Physiology and Pharmacology, The University of Western Ontario, London, Ontario N6A 5C1, Canada

The protein G18 (also known as AGS4 or GPSM3) contains three conserved GoLoco/GPR domains in its central and C-terminal regions that bind to inactive $G\alpha$, whereas the N-terminal region has not been previously characterized. We investigated whether this domain might itself regulate G protein activity by assessing the abilities of G18 and mutants thereof to modulate the nucleotide binding and hydrolytic properties of $G\alpha_{i1}$ and $G\alpha_o$. Surprisingly, in the presence of fluoroaluminate (AlF_4^-) both G proteins bound strongly to full-length G18 (G18wt) and to its isolated N-terminal domain (G18 Δ C) but not to its GoLoco region (Δ NG18). Thus, it appears that its N-terminal domain promotes G18 binding to fluoroaluminate-activated $G\alpha_{i/o}$. Neither G18wt nor any G18 mutant affected the GTPase activity of $G\alpha_{i1}$ or $G\alpha_o$. In contrast, complex effects were noted with respect to nucleotide binding. As inferred by the binding of [³⁵S]GTP γ S (guanosine 5'-O-[γ -thio]triphosphate) to $G\alpha_{i1}$, the isolated GoLoco region as expected acted as a guanine nucleotide dissociation inhibitor, whereas the N-terminal region exhibited a previously unknown guanine nucleotide exchange factor effect on this G protein. On the other hand, the N terminus inhibited [³⁵S]GTP γ S binding to $G\alpha_o$, albeit to a lesser extent than the effect of the GoLoco region on $G\alpha_{i1}$. Taken together, our results identify the N-terminal region of G18 as a novel G protein-interacting domain that may have distinct regulatory effects within the $G_{i/o}$ subfamily, and thus, it could potentially play a role in differentiating signals between these related G proteins.

The classical model of G protein signaling includes three major components: G protein-coupled receptor (GPCR),² heterotrimeric G protein, and effector. The inactive $G\alpha$ subunit binds with high affinity to GPCR, $G\beta\gamma$, and GDP. The binding of an agonist to the receptor promotes its guanine nucleotide exchange factor (GEF) activity toward the G protein that results in the exchange of GDP for GTP. This activates the G protein

and is thought to cause the dissociation of $G\alpha$ and $G\beta\gamma$. Both GTP-bound $G\alpha$ and free $G\beta\gamma$ are capable of initiating signals by interacting with downstream effectors such as adenylyl cyclase, phospholipase $C\beta$, and various ion channels and kinases (1). Signaling is terminated by the intrinsic GTPase activity of the $G\alpha$ subunit, thereby returning the latter to its inactive form and regenerating the inactive $G\alpha\beta\gamma$ complex. It is now recognized that heterotrimeric G protein signaling is more complex than originally proposed, with a number of factors having been identified that can modulate G protein activity. These include the regulator of G protein signaling (RGS) proteins that accelerate G protein deactivation and the receptor-independent activator of G protein signaling (AGS) proteins that modulate G protein signals through several distinct mechanisms. The $G_{i/o}$ -Loco (GoLoco)/G protein regulatory (GPR) motif of the Group II AGS proteins can alter the activities of both $G\alpha$ and $G\beta\gamma$ (2).

The GoLoco/GPR motif was originally identified in the *Drosophila* RGS12 homologue, Loco (3–5). The GoLoco motif is a 19-amino acid sequence that can bind to the $G\alpha$ subunit of $G_{i/o}$ proteins in their inactive state ($G\alpha$ -GDP) to inhibit the exchange of GDP for GTP. This biochemical activity serves as the basis for its function as a guanine nucleotide dissociation inhibitor (GDI) (3, 6–11) to impede $G\alpha$ activation. Several important contact points have been identified between the GoLoco motif and $G\alpha$ subunits, the most notable being the extension of its highly conserved Asp/Glu-Gln-Arg triad into the nucleotide binding pocket of $G\alpha$ that interacts directly with the α - and β -phosphates of GDP (8, 12). This interaction between the GoLoco motif and $G\alpha$ subunits has been shown to promote the dissociation of the $G\beta\gamma$ dimer from $G\alpha$ *in vitro* (12). In this way the GoLoco motif may act as a receptor-independent activator of $G\beta\gamma$ signaling (13–16). The $G\alpha$ -GoLoco complex may also affect physical coupling between $G\alpha$ and the receptor (17, 18), and this may further impact the control of G protein function.

The modulation of G protein activities by GoLoco motif-containing proteins has been implicated in multiple physiological processes. In *Caenorhabditis elegans* and *Drosophila*, GPR1/2 and Pins GoLoco motifs, respectively, have been characterized to play essential roles in asymmetric cell division (5, 19, 20), and analogous mechanisms appear to exist in mammalian systems. For example, the Pins homologue LGN recently was shown to be critical for cell polarization during oocyte meiosis in mice (21). Emerging evidence also points to a role in GPCR signaling. Endogenously expressed LGN, for example, has been found to regulate G protein-dependent GIRK channel function in hippocampal neurons (22), whereas another mam-

* This work was supported by the Canadian Institutes of Health Research.

¹ Holds a Career Investigator Award from the Heart and Stroke Foundation of Ontario. To whom correspondence should be addressed: Dept. of Physiology and Pharmacology, Schulich School of Medicine and Dentistry, University of Western Ontario, London, Ontario N6A 5C1, Canada. Tel.: 519-661-3318; E-mail: peter.chidiac@schulich.uwo.ca.

² The abbreviations used are: GPCR, G protein-coupled receptor; AlF_4^- , fluoroaluminate; GDI, guanine nucleotide dissociation inhibitor; GEF, guanine nucleotide exchange factor; RGS, regulator of G protein signaling; AGS, activators of G protein signaling; GPR motif, G protein regulatory motif; GST, glutathione S-transferase; GTP γ S, guanosine 5'-O-[γ -thio]triphosphate; GAP, GTPase accelerating protein; GoLoco, $G_{i/o}$ -Loco; PMSF, phenylmethylsulfonyl fluoride; Ni-NTA, nickel-nitrilotriacetic acid; DTT, dithiothreitol.

TABLE 1
Primers used for making His-tagged G18 and its mutants

G18wt	Sense primer	5'-gcactccatgatgtcgatggaggctgagagaccccaggaag-3'
	Antisense primer	5'-cgctttaagcttgctcaagtctcagcaggtgtgtgtgg-3'
Δ NG18	Sense primer	5'-gcactccatgatggccatgcagactgaactcctctctggac-3'
	Antisense primer	5'-cgctttaagcttcgactactagttctcagcaggtgtgtgtgg-3'

malian GoLoco protein, Pcp2, is able to modulate receptor regulation of Cav2.1 calcium channels expressed in *Xenopus laevis* oocytes (23).

The current study examines the effects of G18 (AGS4/GPSM3) on G protein activity in a variety of experimental contexts. G18 is a 160-amino acid protein that is composed of three tandem GoLoco motifs interspersed through its middle and C-terminal area plus an uncharacterized N-terminal segment that is rich in proline (14 of 60 residues). Previous biochemical analyses have shown that at least two GoLoco motifs of G18 can interact with GDP-bound $G\alpha_{11}$ both *in vitro* and in overexpressed cell systems (3, 24). However, the overall physiological function of G18 still remains unknown. In the current study we further examine the interactions between G18 and heterotrimeric G proteins, and moreover, we identify its N terminus as a novel G protein-interacting domain.

EXPERIMENTAL PROCEDURES

RNA Preparation and Reverse Transcriptase PCR—Tissues from 3-month-old C57BL/6 mice were collected and homogenized. Total RNA was extracted using Trizol reagent (Invitrogen) and further purified using RNeasy mini columns (Qiagen). 2 μ g of total RNA was used for reverse transcription with the High Capacity Reverse Transcription kit (Applied Biosystems). Primers specific for the open reading frame of G18 were used in PCR reactions to examine the tissue distribution of G18. The level of glyceraldehyde-3-phosphate dehydrogenase was used as loading control.

Preparation of Recombinant Epitope-tagged G18 Fusion Proteins—GST-tagged G18wt (full-length G18), Δ NG18 (an N-terminal 60-amino acid truncation mutant containing only the three GoLoco motifs), and Δ NG18-mGL (lacking the N-terminal 60-amino acid and containing point mutations at the last amino acid of each GoLoco motif from Arg to Phe) were kindly provided by Dr. David P. Siderovski (The University of North Carolina, Chapel Hill, NC). G18-mGL (containing Arg to Phe mutations at the last amino acid of each GoLoco motif) was generated using the site-directed mutagenesis kit (Stratagene). G18 Δ C (the N-terminal domain of G18), which contains only the first 60 amino acids of G18, was generated by inserting a stop codon at the appropriate position. The PCR product was subcloned into the pET-19b or pGEX4T2 vector to generate a His-tagged or GST-tagged fusion protein, respectively. All other constructs of G18 were further subcloned into the pET-19b vector using primers listed in Table 1. Proteins were expressed and purified as described below.

Protein Purification—N-terminal His₁₀-tagged G18 and mutants thereof were purified from *Escherichia coli* BL21 (DE3) strain as follows. Six liters of LB medium containing 100 μ g/ml ampicillin was inoculated with previously transformed cells and grown with vigorous shaking at 37 °C to an $A_{600} \geq 0.5$. Expression of the proteins was induced by the addition of iso-

propyl- β -D-thiogalactopyranoside to a final concentration of 500 μ M and incubated for an additional 4 h before harvesting the bacteria by centrifugation. Bacteria were resuspended in 70 ml of buffer A (25 mM Tris (pH 8.0), 500 mM NaCl, 1% Tween 20, 0.1 mM phenylmethylsulfonyl fluoride (PMSF), 1 μ g/ml leupeptin, 10 μ g/ml aprotinin, and 5 mM imidazole) and incubated on ice with 0.2 mg/ml lysozyme for 30 min. After a further 20-min incubation with 25 μ g/ml DNase I and 0.5 mM $MgCl_2$, 3 ml of a 50% slurry of Ni-NTA affinity resin (Qiagen) pre-equilibrated in buffer A was added, and the mixture was gently rocked at 4 °C for 2 h. The resin was subsequently loaded onto a 30-ml column and washed with buffer B (25 mM Tris (pH 8.0), 500 mM NaCl, 1% Tween 20, 0.1 mM PMSF, 1 μ g/ml leupeptin, 10 μ g/ml aprotinin, 20 mM imidazole) followed by buffer C (25 mM Tris (pH 8.0), 500 mM NaCl, 0.2 mM PMSF, 2 μ g/ml leupeptin, 20 μ g/ml aprotinin, 40 mM imidazole). Proteins were eluted from the Ni-NTA beads by adding 800 μ l of buffer D (final concentrations: 25 mM Tris (pH 8.0), 500 mM NaCl, 0.2 mM PMSF, 1 μ g/ml leupeptin, 10 μ g/ml aprotinin, 250 mM imidazole) after a 30-min incubation at 4 °C. This process was repeated a total of six times. This procedure yielded proteins that were ~60% pure as determined by Coomassie Blue staining. Samples were further purified by fast protein liquid chromatography using a Superdex 75 column (GE Healthcare) to yield proteins that were >90% pure. Peak fractions were pooled and stored in aliquots at -80 °C.

GST-tagged G18 proteins were purified using a previously established glutathione-Sepharose 4B affinity purification method (25). His-tagged $G\alpha_{11}$ and $G\alpha_o$ were grown in enriched medium (2% Tryptone, 1% yeast extract, 0.2% glycerol, 0.5% NaCl, 50 mM KH_2PO_4), induced with 30 μ M isopropyl- β -D-thiogalactopyranoside, and purified as described previously (26).

Protein-Protein Interaction Assay—Purified His₆- $G\alpha_{11}$ or His₆- $G\alpha_o$ (500 nM) was preincubated for 1 h in binding buffer (50 mM Tris (pH 7.5), 0.6 mM EDTA, 150 mM NaCl, 1 mM DTT, 0.1% Triton X-100, PMSF 2 μ g/ml leupeptin, and 20 μ g/ml aprotinin) at 30 °C in the presence of either 10 μ M GDP or GDP+AMF (10 mM NaF, 10 mM $MgCl_2$, 20 μ M $AlCl_3$). An equimolar amount (500 nM) of GST-tagged G18WT, G18-mGL, Δ NG18, Δ NG18-mGL, or G18 Δ C was added to the $G\alpha$ mixture and incubated on a rotating platform at 4 °C for 2 h. Glutathione-Sepharose 4B beads or Ni-NTA-agarose beads (20 μ l bed volume) were then added into the protein mixture and incubated overnight. The protein mixture was washed three times with binding buffer in the presence of GDP with/without AMF, and the beads were resuspended in 2 \times Laemmli buffer. Eluted proteins were separated on a 12% SDS gel and transferred to a polyvinylidene fluoride transfer membrane (Pall Corp.) for immunoblotting.

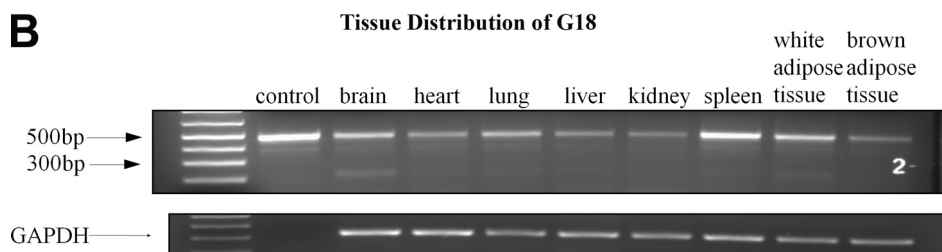


FIGURE 1. *A*, shown is the amino acid sequence of G18. The three GoLoco motifs are *underlined*. The proline residues are shown in *white on a black background*, and arginines that could potentially contribute to the N-terminal effects are indicated in *bold type*. *B*, tissue distribution of G18 is shown. Various tissues from 3-month-old C57BL/6 mice were isolated, total RNA was extracted, and reverse transcriptase-PCR followed by PCR was performed using primers specific for the open reading frame of G18. Glyceraldehyde-3-phosphate dehydrogenase (*GAPDH*) was used as a loading control. The control lane indicates the reference length of G18 using the PCR product from the plasmid.

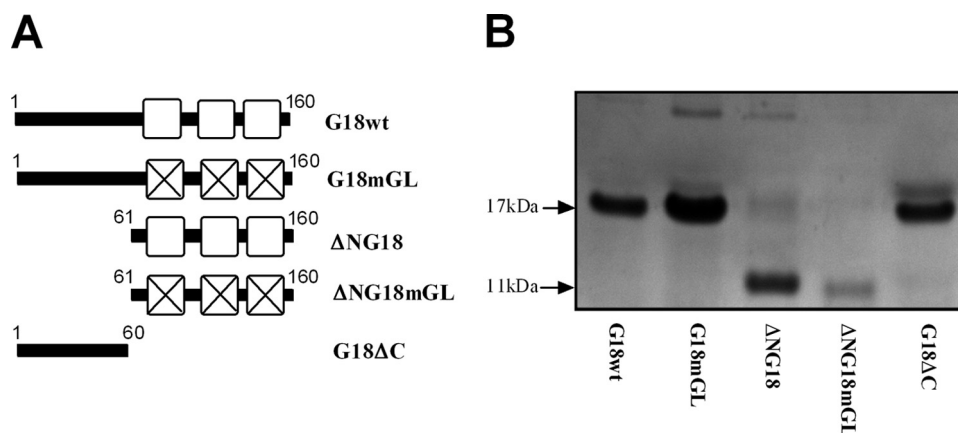


FIGURE 2. **Constructs and purified proteins.** *A*, shown is the domain architecture of different constructs used in the study. *B*, His-tagged proteins were purified from *E. coli* strain BL21 (DE3) using Ni-NTA affinity purification followed by fast protein liquid chromatography. Protein purity was estimated by Coomassie staining. The correct molecular size of G18ΔC (which may have run anomalously due to its high proline content) was verified by mass spectrometry.

Immunoblotting—Membranes were incubated with blocking buffer (Tris-buffered saline Tween 20 (TBST) with 5% skim milk) for 1 h and then probed with anti-His or anti-GST antibody (1:1000) (Santa Cruz biotechnology) diluted in blocking buffer overnight on a rotating platform at 4 °C. Blots were subsequently washed 3 times with TBST and then incubated with horseradish peroxidase-conjugated secondary antibody (1:2000) (Promega) diluted in TBST for 1 h at room temperature. After another three washes with TBST, the blot was visualized by LumiGLO Reserve chemiluminescence substrate (KPL, Inc.) using a FluorChem 8000 imaging system.

Presteady State GTPase Assay—Presteady state GTPase activity of purified G proteins was measured as described earlier (26). Purified His₆-Gα₁₁ or His₆-Gα_o (1 μM) was incubated with [γ-³²P]GTP (1 × 10⁶ cpm/assay) plus 1 μM nonradioactive GTP for 15 min at 30 or 20 °C in GTP binding buffer (50 mM Hepes (pH 7.5), 0.05% Lubrol, 1 mM DTT, 10 mM EDTA, 5 μg/ml

bovine serum albumin) and then kept on ice. The GTP binding reaction was stopped by the addition of 0.25 volumes of mix buffer (50 mM Hepes (pH 7.5), 10 mM MgCl₂, 500 μM GTP), and a single round of GTP hydrolysis was initiated by adding 10 mM Mg²⁺ in the presence or absence of 1 μM G18, one of its mutants, RGS4 (300 nM in Fig. 5, 100 nM in Fig. 8), or both RGS4 and G18. Aliquots were taken at the indicated time points and quenched with ice-cold 5% (w/v) Norit in 0.05 M NaH₂PO₄. The level of radioactive ³²P_i in the supernatant was detected by liquid scintillation counting on a Packard Tri-Carb 2900TR liquid scintillation counter (PerkinElmer Life Sciences).

Presteady State GTPγS Binding Assay—Purified His₆-Gα₁₁ (100 nM) or His₆-Gα_o (100 nM) was incubated for 1 h at 4 °C in binding buffer (20 mM Hepes (pH 8.0), 1 mM EDTA (pH 8.0), 100 mM NaCl, 1 mM DTT, 2 mM MgCl₂, 0.1 mg/ml bovine serum albumin, 0.1% Lubrol, PMSF, 1 μg/ml leupeptin, and 10 μg/ml aprotinin) in the presence or absence of 1–2 μM G18 or its mutants. Binding assays were initiated by adding 0.5 μM [³⁵S]GTPγS (1.25 × 10⁵ cpm/pmol). The incubation continued for 30 min at 30 °C (Gα₁₁) or 60 min at 20 °C (Gα_o). The assay was terminated by adding ice-cold stop buffer (20 mM Tris (pH 8.0), 10 mM MgCl₂, 100 mM NaCl, 0.1% Lubrol, 1 mM GTP, and 0.1 mM DTT). Samples were filtered

through nitrocellulose membranes (Millipore) followed by washing four times with 2 ml of ice-cold wash buffer (20 mM Tris (pH 8.0), 100 mM NaCl, 10 mM MgCl₂). Radioactivity was measured using liquid scintillation counting. The nonspecific binding was determined in the presence of 100 μM unlabeled GTPγS, and these values were subtracted to yield specific binding.

Solution-based Steady State GTPase Assay—Purified His₆-Gα₁₁ or His₆-Gα_o (250 nM) was incubated with 3 μM G18 or one of its mutants for 30 min at 4 °C in assay buffer (50 mM Na-Hepes (pH 8.0), 1 mM EDTA, 2 mM DTT, 0.1% Triton X-100, 6 mM MgSO₄, protease inhibitor, PMSF). [γ-³²P]GTP (1 × 10⁶ cpm/assay) plus 5 μM nonradioactive GTP was then added, and the protein mix was further incubated for 1 h at 30 °C (Gα₁₁) or 20 °C (Gα_o). The reaction was stopped by adding ice-cold 5% (w/v) Norit in 0.05 M NaH₂PO₄. After centrifugation, the level of radioactive ³²P_i in the supernatant was determined by liquid scintillation counting.

Receptor- and Agonist-stimulated GTPase Assay—Sf9 membranes overexpressing M2 muscarinic receptor and heterotrimeric G proteins were prepared as indicated previously (27). These Sf9 cell membranes (8 μ g/tube) were assayed for 100 μ M carbachol-stimulated GTP hydrolysis at 30 °C for 5 min in the absence or presence of the indicated purified proteins in the reaction buffer (20 mM Hepes (pH 7.5), 1 mM EDTA, 1 mM

DTT, 0.1 mM PMSF, 10 mM NaCl, 2 mM MgCl₂ (7.5 mM free Mg²⁺), 1 μ M GTP, 1 mM ATP, [γ -³²P]GTP (1 \times 10⁶ cpm per assay), and protease inhibitors) in a total reaction volume of 50 μ l. The assay was stopped by adding 950 μ l of ice-cold 5% (w/v) Norit in 0.05 M NaH₂PO₄. The reaction mixture was centrifuged, and the level of ³²P_i in the resulting supernatant was determined by liquid-scintillation counting. The nonspecific GTPase activity was defined as that in the presence of the inverse agonist tropicamide (10 μ M), and these values were subtracted from the total counts per minute to yield the agonist- and receptor-dependent GTP hydrolysis.

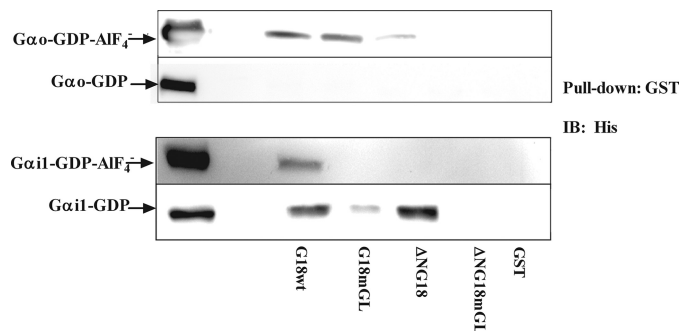


FIGURE 3. Protein-protein interaction between G proteins and G18. Purified His₆-G α_{i1} or G α_o was incubated with excess GDP \pm AlF₄⁻ for 30 min at 4 °C, purified GST-tagged G18 or one of its mutants was added to the solution, and the incubation was continued for another 2 h before adding glutathione-Sepharose 4B beads. After overnight incubation at 4 °C on a rotating platform, the mixture was centrifuged and washed, and the resulting pellet was retained for immunoblotting (IB) analysis. Membranes were probed with anti-His antibody. *Input* represents 10% of the protein used in the pulldown assay. A representative blot of three independent experiments is shown.

RESULTS

Tissue Distribution of G18 in Mice—G18 is a 160-amino acid protein encoded by a 1472-bp mRNA with 88% similarity between human and mice at the amino acid level (3). To determine the tissue distribution of G18 in mice, total RNA was extracted from different tissues of 3-month-old C57BL/6 mice, and primers specific for the open reading frame of G18 were used to probe for G18. As shown in Fig. 1, full-length G18 was detected at ~500 bp, corresponding well to the open reading frame of 480 bp. We found that G18 was highly expressed in spleen and lung and moderately expressed in heart, kidney, liver, brain, and adipose tissue. These results are consistent with a previous report by Cao *et al.* (3) using a human RNA blot, thus indicating a similar tissue distribution between human and mouse.

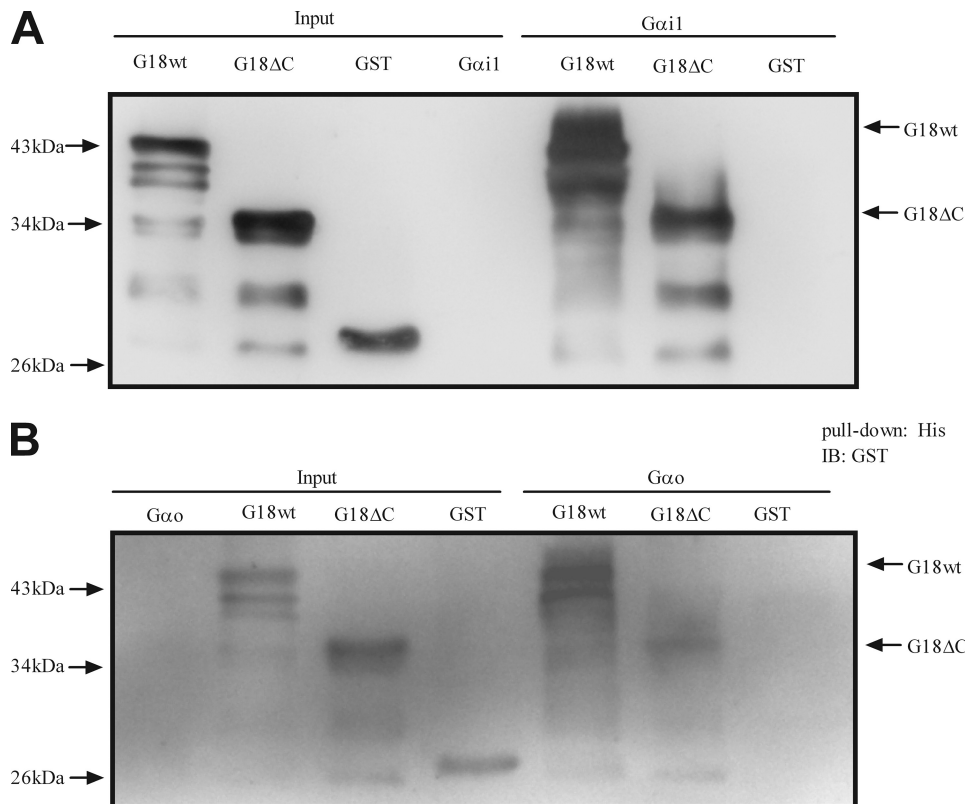


FIGURE 4. Protein-protein interaction between G proteins and the N terminus of G18. Purified His₆-G α_{i1} or G α_o was incubated with excess GDP + AlF₄⁻ for 30 min at 4 °C, purified GST-tagged G18 or its isolated N terminus (G18 Δ C) was added to the solution, and the incubation was continued for another 2 h before adding Ni-NTA-agarose beads. The protein mix was further incubated overnight at 4 °C on a rotating platform, samples were centrifuged, and the resulting pellet was retained for immunoblotting (IB) analysis. Membranes were probed with anti-GST antibody. *Input* represents 10% of the protein used in the pulldown assay. A representative blot of three independent experiments is shown.

Purified G18 Can Interact with Both Inactive and Fluoroaluminate-activated G α Proteins—Previous studies have shown that the GoLoco motifs of G18 have higher binding affinity toward G α_i -GDP compared with G α_o -GDP (3, 24). To extend these findings, we tested the binding between purified G18 and purified G α_{i1} or G α_o in both their inactive GDP-bound and fluoroaluminate-activated states. Three G18 mutants were examined (Fig. 2) that contain an N-terminal truncation (Δ NG18), inactivating point substitutions within each GoLoco motif (G18-mGL), or a combination of both modifications (Δ NG18-mGL). Consistent with previous studies (3, 24), G18wt and Δ NG18 interacted with G α_{i1} -GDP, whereas G18-mGL and Δ NG18-mGL did not (Fig. 3). None of the purified G18 proteins displayed any detectable binding to the GDP-bound form of G α_o under the conditions employed in our studies (Fig. 3).

To determine whether the observed G18 interactions were specific for inactive G protein, we performed parallel *in vitro* pulldown

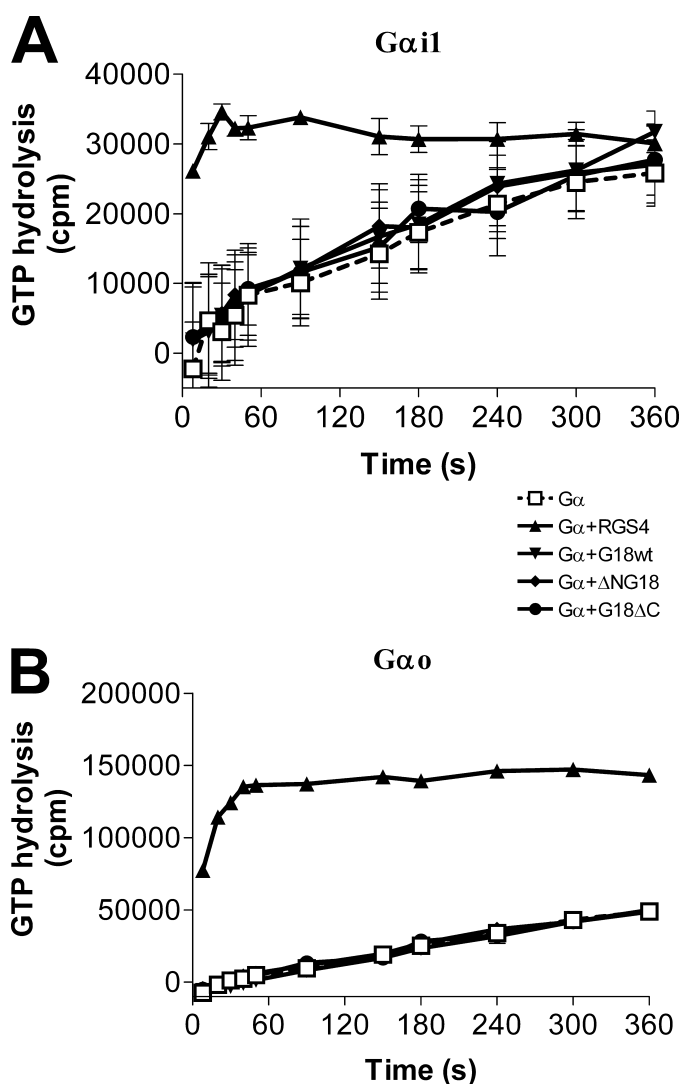


FIGURE 5. The effects of G18 on G protein GTPase activity under presteady state conditions. Purified His₆-Gα_{i1} (A) or His₆-Gα_o (B) was incubated with [³²P]GTP (1 × 10⁶ cpm/assay) for 15 min at 30 °C (Gα_{i1}) or 20 °C (Gα_o). A single round of GTP hydrolysis was measured at 0 °C in the presence of 10 mM Mg²⁺ and RGS4, G18, or one of its mutants as indicated. Data points shown are the means ± S.E. from three independent experiments.

assays in the presence of AlF₄⁻ to mimic the transition state of G protein. Surprisingly, in the presence of AlF₄⁻, both Gα_{i1} and Gα_o interacted with G18wt (Fig. 3). Moreover, removal of the G18 N-terminal domain diminished its binding to G proteins (Fig. 3). These results suggest that whereas the GoLoco motifs of G18 are responsible for its interaction with inactive Gα_i, the N-terminal segment of G18 may serve to bind the fluoroaluminate-activated Gα_{i/o}.

The N-terminal Domain of G18 Can Interact with Fluoroaluminate-activated Gα Proteins—We also generated and tested an additional truncation mutant of G18 containing only the first 60 residues (G18ΔC) to confirm the binding between the N terminus of G18 and the transition state of G proteins. Indeed, this segment of G18 was sufficient to bind to fluoroaluminate-activated forms of both Gα_{i1} and Gα_o (Fig. 4).

G18 Has No Effect on G Protein GTPase Activity in Presteady State GTPase Assays—We examined the effects of G18wt, ΔNG18, and G18ΔC on the various stages of the G protein

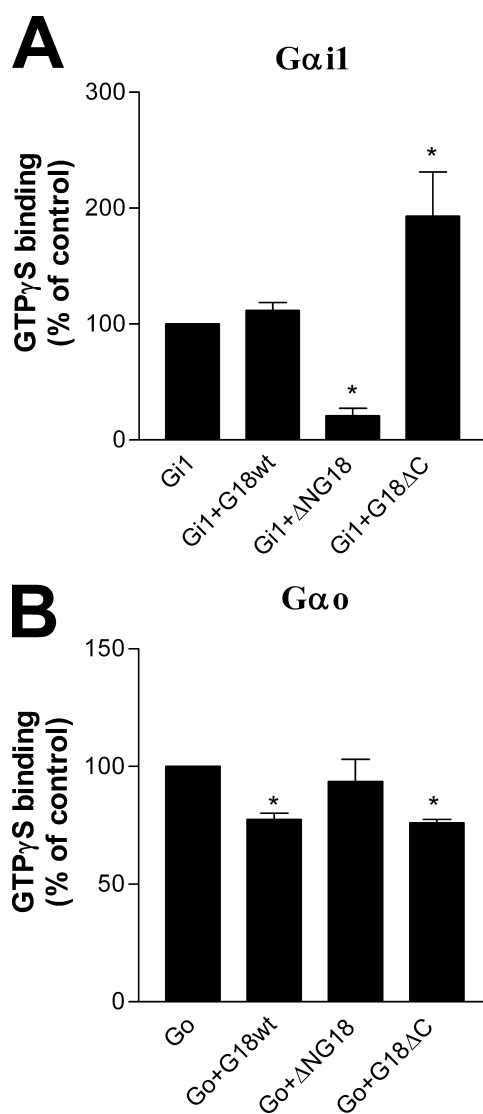


FIGURE 6. The effects of G18 on G protein nucleotide exchange. Purified His₆-Gα_{i1} (A) or His₆-Gα_o (B) was preincubated with G18 at 4 °C. Binding assays were initiated by adding 0.5 μM [³⁵S]GTPγS (1.25 × 10⁵ cpm/pmol) at 30 °C (Gα_{i1}) or 20 °C (Gα_o). The binding of GTPγS to Gα proteins was measured after 30 min (Gα_{i1}) or 60 min (Gα_o) of incubation. Nonspecific binding was estimated in the presence of excess unlabeled GTPγS, and these values were subtracted from the results. The data are presented as the mean ± S.E. of three to five independent experiments performed in duplicate. *, *p* < 0.05, compared with G protein alone (one-way analysis of variance with Tukey's multiple comparison test).

guanine nucleotide binding cycle to determine the biochemical significance of the interaction between the G18 N terminus and Gα subunits. Because GTPase-activating proteins (GAP) tend to have high affinity for fluoroaluminate-activated G proteins (28, 29), we first investigated the possibility that the G18 N terminus might have GAP activity toward Gα_{i/o} subunits using a solution-based presteady state GTPase assay.

Our results revealed that none of the purified G18 proteins tested had any impact on the rate of GTP hydrolysis by Gα_{i1} or Gα_o (Fig. 5). RGS4, serving as a positive control, exhibited robust GAP activity on both Gα_{i1} and Gα_o (Fig. 5). These results indicate that G18 does not serve as a GAP toward free Gα_{i/o} subunits.

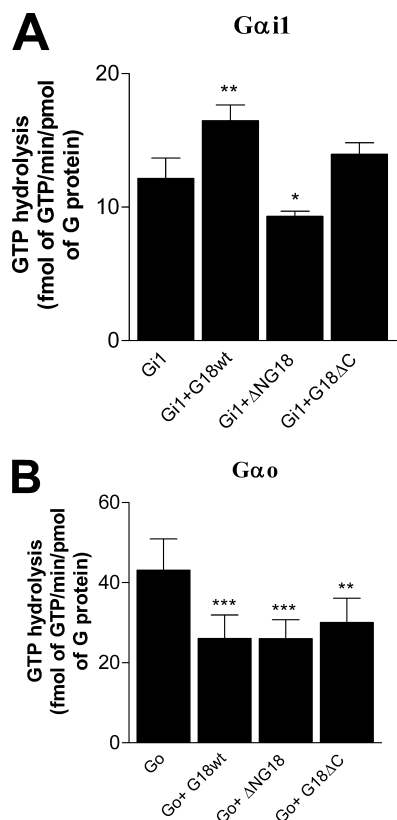


FIGURE 7. The effects of G18 on G α protein GTPase activity under steady state conditions. Purified His₆-G α_{i1} (A) or His₆-G α_o (B) was mixed with G18 at 4 °C. The protein mixture was incubated with [γ -³²P]GTP (1×10^6 cpm/assay) in the presence of 6 mM Mg²⁺ at 30 °C (G α_{i1}) or 20 °C (G α_o). The free ³²P_i level was measured after 60 min of incubation. The data are presented as the mean \pm S.E. of three independent experiments performed in duplicate. *, $p < 0.05$; **, $p < 0.01$; ***, $p < 0.001$ compared with G protein alone (one-way analysis of variance with Tukey's multiple comparison test).

The N-terminal Domain of G18 Acts as a GEF on G α_{i1} —We next assessed whether the N terminus of G18 might have any effects on nucleotide exchange distinct from the established GDI activity of its GoLoco motifs on G α_i proteins. Changes in the rate of GDP dissociation from G α proteins were inferred from changes in the rate of GTP γ S binding using a solution-based presteady state assay. As expected, the GoLoco region of G18 (Δ NG18) acted to inhibit GDP dissociation from G α_{i1} , as revealed by an 85% decrease in GTP γ S binding to the latter (Fig. 6A). In contrast, the isolated N-terminal segment of G18 (G18 Δ C) increased GTP γ S binding to G α_{i1} by \sim 60%. Interestingly, full-length G18 had essentially no effect on the observed rate of GTP γ S binding to G α_{i1} , suggesting that the opposing functions of the two domains balance out under these experimental conditions. These results suggest that G18 can serve as a bifunctional regulator of G α_{i1} whereby its GoLoco region functions as a GDI and its N-terminal domain acts as a GEF.

We further used a solution-based, steady state GTPase assay to corroborate the putative GEF activity of the G18 N-terminal region on G α_{i1} . Interestingly, full-length G18 significantly promoted GTP turnover (Fig. 7A). In contrast, the N-terminal deletion mutant Δ NG18 decreased GTPase activity (Fig. 7A), which is consistent with its GDI activity. In agreement with the results obtained from presteady state GTP γ S binding assays (Fig. 6A), there was a trend toward an increase with G18 Δ C

(Fig. 7A), and this reached statistical significance when the concentration was raised to 10 μ M (data not shown). These results suggest that under steady state conditions with free G α_{i1} , the GEF activity of the N-terminal domain of G18 predominates over the GDI function of its GoLoco region.

The N-terminal Domain of G18 Acts as a GDI on G α_o —The effects of G18 and its mutants on G α_o activity were also examined. Surprisingly, G18wt inhibited nucleotide exchange on free G α_o by \sim 25% (Fig. 6B). The GoLoco region of G18 (Δ NG18) had no effect on GDP dissociation from G α_o , which is consistent with its poor binding to G α_o -GDP. In contrast, G18 Δ C inhibited GTP γ S binding to G α_o to the same level as G18wt. These results indicate that G18 has a modest albeit statistically significant GDI effect on G α_o , which appears to be primarily attributable to its N-terminal domain.

Furthermore, in the solution-based steady state GTPase assay, both G18wt and G18 Δ C decreased the GTP hydrolysis of free G α_o , consistent with the observed GDI effects of the full-length protein and the isolated N-terminal domain (Fig. 7B). Δ NG18 also inhibited the GTPase activity of G α_o under these conditions. The reason for the apparent discrepancy regarding the effects of Δ NG18 in Fig. 6B versus Fig. 7B is not clear. Overall our results suggest that the function of the N-terminal domain of G18 may depend on which G protein is involved, *i.e.* promoting nucleotide exchange at G α_{i1} but inhibiting at G α_o .

Effects of G18 on Receptor- and Agonist-stimulated G Protein GTPase Activity—The foregoing observations indicate that the activity of G18 is not limited to its GoLoco motifs, as its N-terminal domain also modulates G protein-nucleotide interactions. In addition, these results clearly identify G α_o as a novel interacting partner of G18. However, little is known regarding the activity of G18 (and GoLoco motif-containing proteins in general) within the context of receptor-stimulated G protein function. Therefore, we used a receptor- and agonist-dependent steady state GTPase assay to study the effects of G18 on GTP turnover by overexpressed G α_{i1} or G α_o in membranes from Sf9 cells also co-expressing exogenous M2 muscarinic receptor and G $\beta\gamma$ subunits.

The addition of G18wt to carbachol-activated M2+G α_{i1} or M2+G α_o membranes yielded little or no change in agonist-dependent GTPase activity (Fig. 8, A and B), notwithstanding its demonstrated effects in solution-based assays. Mutant forms of G18 similarly lacked activity under these conditions (data not shown). This apparent lack of effect could reflect a masking of changes in nucleotide exchange rates by the relatively slow intrinsic hydrolytic activities of G α_{i1} and G α_o in the presence of the receptor. To ensure that GTP hydrolysis *per se* was not rate-limiting, cyclical GTP turnover was also measured in the presence of purified RGS4, which accelerates the hydrolytic step (Fig. 5). Indeed, the inclusion of RGS4 in these assays revealed effects of G18wt on both G α_{i1} and G α_o , which were inhibited, respectively, by \sim 60 and 80% at the maximally obtainable concentration of G18wt (Fig. 8, A and B). Another conceivable explanation is that this observation may reflect an effect of G18 on RGS4 activity. We used a presteady state GTPase assay to test this possibility and found that G18 had little or no effect on the GAP activity of RGS4 on either G α_{i1} or G α_o (Fig. 8, C and D).

Novel Regulatory Function of G18

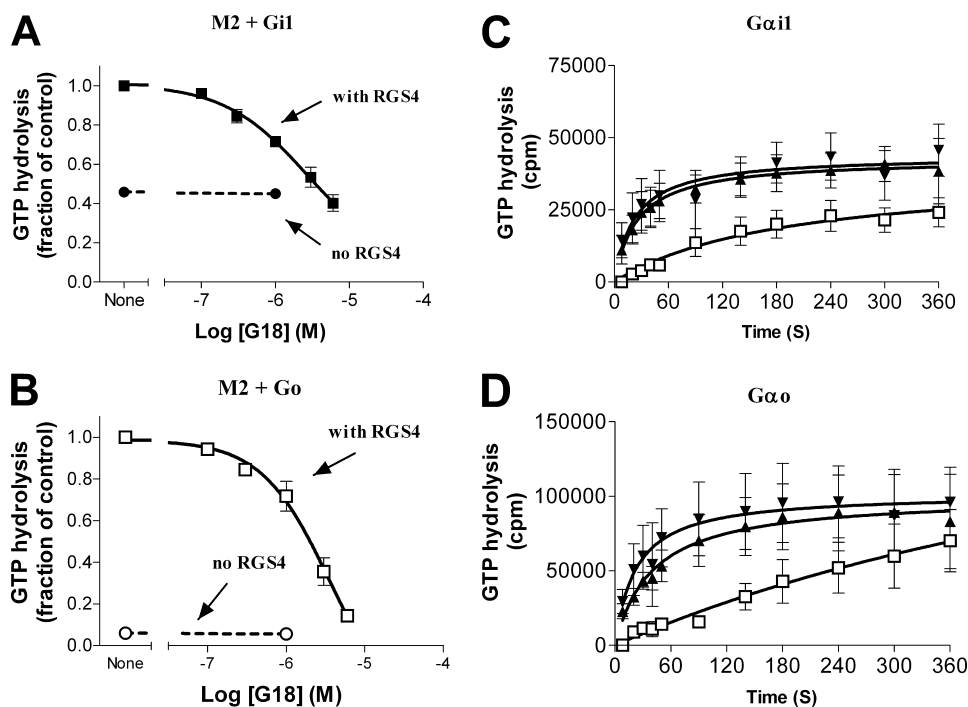


FIGURE 8. The effects of G18 on receptor- and agonist-stimulated G protein GTPase activity. A and B, Sf9 cell membranes overexpressing M2 muscarinic acetylcholine receptor and heterotrimeric G_{α₁₁} or G_{α_o} were prepared as indicated under "Experimental Procedures." Carbachol was used to activate M2 receptor. Steady state GTPase activities of G proteins were measured in the presence (solid line) or absence (dashed line) of RGS4 and the indicated concentrations of G18wt. Nonspecific signal was determined in the absence of added purified proteins and in the presence of tropicamide. The data are presented as the mean ± S.E. of three-four independent experiments. C and D, purified His₆-G_{α₁₁} or His₆-G_{α_o} was incubated with [³²P]GTP (1 × 10⁶ cpm/assay) for 15 min at 30 °C (G_{α₁₁}) or 20 °C (G_{α_o}). A single round of GTP hydrolysis was measured at 0 °C in the presence of 10 mM Mg²⁺ (□) and RGS4 (▲) or RGS4+G18 (▼). Data points shown are the means ± S.E. from three independent experiments.

To determine which regions of G18 might contribute to its effects on receptor-stimulated GTP turnover by G₁₁ and G_o, mutants bearing truncations and/or inactivating GoLoco point substitutions were also evaluated. Compared with full-length G18wt, N-terminal-truncated G18 (ΔNG18) produced a similar inhibitory effect on receptor-activated G₁₁ (Fig. 9A) but a greatly reduced effect on G_o (Fig. 9B). In contrast, mutation of the GoLoco motifs (G18-mGL) substantially reduced activity on G₁₁ (Fig. 9C) but caused only a minor change in the inhibitory effect of G18 on G_o GTPase activity (Fig. 9D). Despite the evident GEF effect of G18ΔC on isolated G_{α₁₁} in solution (Fig. 6A), such activity was not observed in membranes in the presence of agonist-activated receptor plus Gβγ (Fig. 9E), suggesting that the GEF activity of the receptor may exceed that of the N-terminal domain of G18. G18ΔC instead produced a marginal inhibitory effect on receptor-activated G₁₁ (Fig. 9E) and a more pronounced inhibitory effect in corresponding experiments with G_o (Fig. 9F). The latter observation reinforces the notion that G18ΔC has the potential to act as a GDI toward G_{α_o}. Overall, the inhibitory effect of full-length G18 on M2+G₁₁ GTPase activity is attributable primarily to its GoLoco motifs, whereas the effect on M2+G_o seems to derive mostly from its N-terminal domain.

DISCUSSION

G18 was first identified within the major histocompatibility complex class III region on chromosome 6 and, thus, may be

involved in the control of host immune defense and inflammatory responses (30, 31). Such a role is further suggested by its relatively high expression levels in the spleen (Fig. 2) and other immune tissues (3), although overall it appears to be fairly widely distributed. Little is known about the biological function of G18, and a clear understanding of this is difficult without accurate knowledge of its biochemical behavior. The most significant finding described herein is the identification of the N-terminal region of G18 as a novel binding partner of G_{α_{i/o}} proteins. Surprisingly, this domain acts as a GEF on G_{α₁₁} but as a weak GDI on G_{α_o}. To our knowledge, this is the first example of a single domain that has distinct regulatory effects toward different Gα proteins. Another unusual property of G18 is that it contains multiple G protein binding domains that produce dissimilar effects on the activity of a common target, and the ability of G18 both to promote and impede GDP dissociation from G_{α₁₁}, respectively, via its N-terminal and GoLoco regions appears to

be unique. A comparable enigma exists with the R12 subfamily of RGS proteins, most of which contain a GoLoco motif that can produce GDI effects on G_{α_i} and also an RGS domain that accelerates GTPase activity (7).

The most widely recognized GEF effects on heterotrimeric G proteins are those produced by agonist-activated GPCRs, but beyond this classical paradigm a variety of non-receptor GEFs has also been identified including Ric-8A (32, 33), Ric-8B (34), CSPα (35), GIV (36), AGS1/Dexas1 (37), GAP-43/neuro-modulin/B-50 (38), and the yeast protein Arr4 (39). The primary amino acid composition of the N-terminal domain of G18 does not resemble any of the previously identified GEFs; however, there are structural attributes of G18 that could conceivably contribute to interactions with G proteins. For example, the N-terminal segment of G18 is highly enriched in proline (14 of 60 residues), which has a special role in protein function due to its unique side chain structure and its effects on overall protein conformation. Proline residues tend to disrupt both α-helical and β-sheet structures, and two or more residues in a row typically promote left-handed PPII (polyproline type II) helices containing three residues per turn (40, 41). PPII helices can readily adopt different conformations and, thus, bind to a variety of proline recognition domains, such as SH3 and WW domains (40). Proline-rich motifs have been found within several effectors of monomeric G proteins, such as Son of sevenless (42, 43), Sprouty 2 (42, 44), and POB1 (42, 45). Our results suggest that a proline-rich motif may also serve as a binding

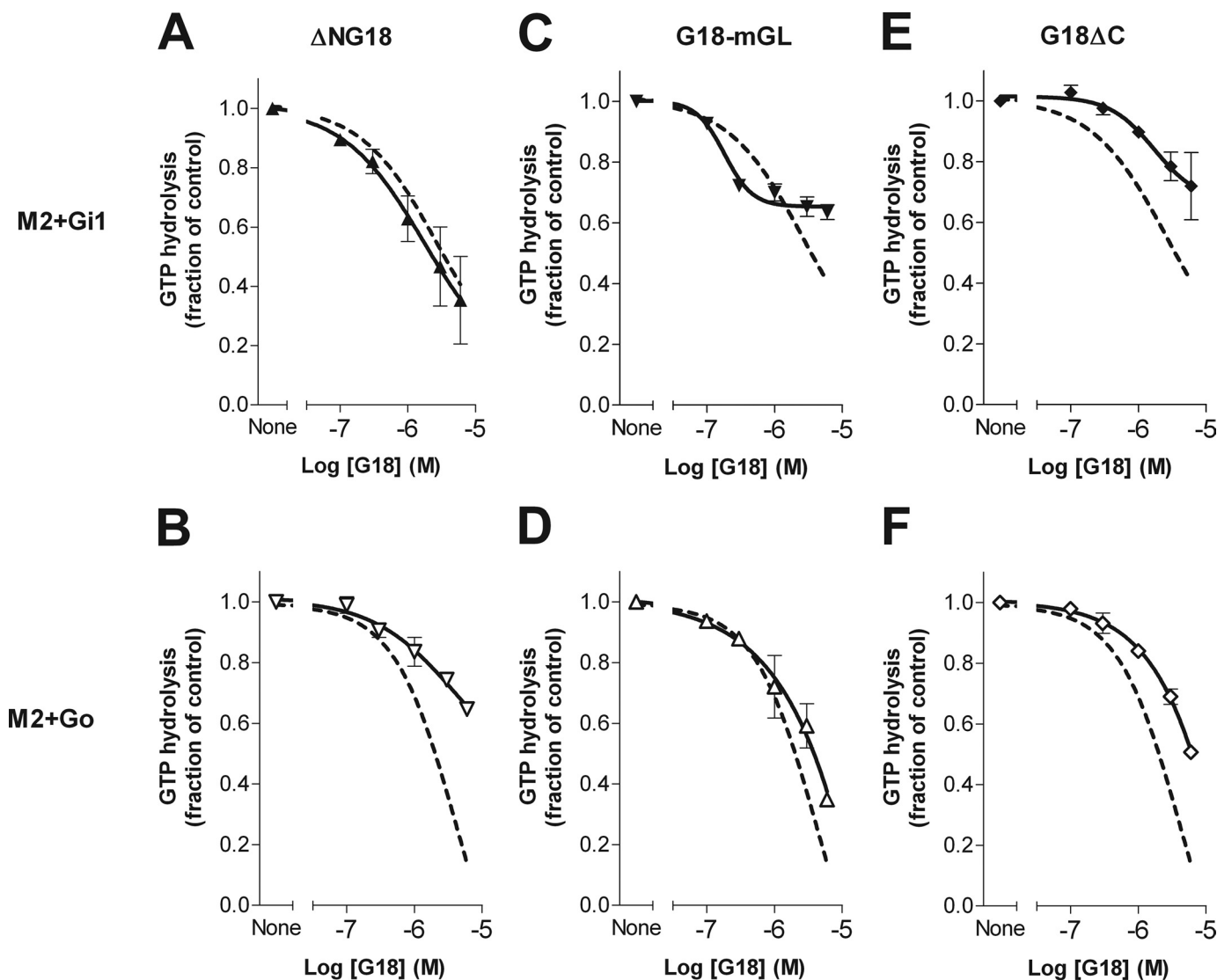


FIGURE 9. The effects of G18 mutants on receptor- and agonist-stimulated G protein GTPase activity. M2-G₁₁ and M2-G_o membranes from sf9 cells were assayed for agonist-stimulated steady state GTPase activity in the presence of RG54 and the indicated concentrations of G18 mutants, as described in Fig. 7. G18wt activity (Fig. 7) is shown as a dashed line for comparison in each panel. The data points shown are means \pm S.E. from three to four independent experiments.

partner for heterotrimeric G proteins. The mechanism by which G18 confers GEF activity on free G α_{11} requires further study, but the presence of multiple arginine residues, particularly those at positions 31, 34, and 46 (which would line up in a PPII helix), could conceivably provide the cationic interface needed to promote nucleotide exchange (46).

Consistent with the present results, previous studies have shown the GoLoco region of G18 to selectively bind to and impede GDP dissociation from inactive G α_i (3, 24). However, the GoLoco motifs in proteins such as Pcp2 and Rap1GAP appear not to be selective between G α_i and G α_o (10, 47, 48). Also it is not obvious that the potential effects of activating agents have necessarily been tested in all studies on GoLoco-G α interactions. The present results indicate that the binding of the GoLoco region of G18 to G α_o can be induced, albeit modestly, by AlF₄⁻ (Fig. 3, fourth lane). Nothing analogous to this observation could be found in the literature; however, the *Drosophila* GoLoco protein Pins has been shown to bind to both active and

inactive G α_o (in this case *Drosophila* G α_o purified from bacteria) and to regulate G α_o -dependent GPCR signaling (49). Although we and Kimple *et al.* (24) were unable to show binding between non-activated mammalian G α_o and the GoLoco region of G18, Cao *et al.* (3) did observe binding to G α_o -GDP. The latter study used G α_o purified from insect cells rather than *E. coli*, suggesting that co- and/or post-translational modification of G proteins may affect their GoLoco interactions.

All of the G protein binding functions of G18 appear to be sensitive to the activation states of their G α targets (Fig. 3). N-terminal domain binding seems to be selective for the transition state of both G α_{11} and G α_o . These interactions appear to be of primary importance for the binding of full-length G18wt in the presence of AlF₄⁻, as G protein binding was greatly reduced or eliminated in the absence of the N-terminal domain. However, both the GEF (on G α_{11}) and GDI (on G α_o) functions of the N-terminal domain of G18 must ultimately be viewed within the context of the entire protein, including its three

Novel Regulatory Function of G18

GoLoco motifs. Important considerations include 1) which, if any, domain has a predominant effect on a particular G protein either as it signals at the plasma membrane or performs other functions in the cell interior, 2) whether G protein binding is mutually exclusive or can occur simultaneously to both the N-terminal domain and one of the GoLoco motifs, and 3) whether an individual G protein can bind to different G18 domains at different points within its GTPase cycle.

The effect of G18 on a G protein may depend on its cellular localization and/or other binding partners. We observed that the N-terminal GEF effect negates (Fig. 6A) or overrides (Fig. 7A) the GoLoco GDI effects on $G\alpha_{i1}$ in solution, whereas the ability of G18 to inhibit receptor-stimulated G_{i1} activity is unaffected by the removal of the N-terminal domain (Fig. 9A). This suggests that perhaps free intracellular $G\alpha_{i1}$ would be activated by the N-terminal GEF function of G18, whereas the GoLoco motifs would inhibit receptor-dependent $G\alpha_{i1}$ activation at the plasma membrane.

Together, the four G protein binding functions within G18 have the potential to produce complex effects on G protein activity. It is unclear whether the N-terminal and GoLoco domains might either impede or facilitate the other's binding to $G\alpha$ or whether the different domains can act sequentially as $G\alpha$ goes through its GTP cycle. If they act independently, then multiple G proteins could be affected at the same time. Kimple *et al.* (24) have shown that the first and third GoLoco motifs within N-terminal-truncated G18 can simultaneously bind individual G proteins and, thus, function as independent GDIs, although this could potentially differ in the presence of other G protein regulators. The idea that the N-terminal domain might be able to access GoLoco-associated $G\alpha$ is suggested by evidence that Ric-8A can exert its GEF activity on $G\alpha_i$ while the latter is coupled to the GoLoco region of AGS3 (33). Analogously, GPCRs and $G\beta\gamma$ must act in concert for agonist-stimulated nucleotide exchange to occur (50–52). Although it is an intriguing possibility, the present results do not directly speak to whether the N-terminal and GoLoco domains of G18 might bind simultaneously to either $G\alpha_{i1}$ or $G\alpha_o$ (or alternatively inhibit one another), and thus, further studies will be required to address this issue.

Acknowledgments—We thank Dr. David P. Siderovski (The University of North Carolina, Chapel Hill, NC) for providing G18 constructs. We also thank Dr. Ken Yeung and Kristina Jurcic (University of Western Ontario) for performing the mass spectrometry study.

REFERENCES

1. Neves, S. R., Ram, P. T., and Iyengar, R. (2002) *Science* **296**, 1636–1639
2. Blumer, J. B., Smrcka, A. V., and Lanier, S. M. (2007) *Pharmacol. Ther.* **113**, 488–506
3. Cao, X., Cismowski, M. J., Sato, M., Blumer, J. B., and Lanier, S. M. (2004) *J. Biol. Chem.* **279**, 27567–27574
4. Siderovski, D. P., Diversé-Pierluissi, M., and De Vries, L. (1999) *Trends Biochem. Sci.* **24**, 340–341
5. Willard, F. S., Kimple, R. J., and Siderovski, D. P. (2004) *Annu. Rev. Biochem.* **73**, 925–951
6. De Vries, L., Fischer, T., Tronchère, H., Brothers, G. M., Strockbine, B., Siderovski, D. P., and Farquhar, M. G. (2000) *Proc. Natl. Acad. Sci. U.S.A.* **97**, 14364–14369

7. Kimple, R. J., De Vries, L., Tronchère, H., Behe, C. I., Morris, R. A., Gist, Farquhar, M., and Siderovski, D. P. (2001) *J. Biol. Chem.* **276**, 29275–29281
8. Kimple, R. J., Kimple, M. E., Betts, L., Sondek, J., and Siderovski, D. P. (2002) *Nature* **416**, 878–881
9. McCudden, C. R., Willard, F. S., Kimple, R. J., Johnston, C. A., Hains, M. D., Jones, M. B., and Siderovski, D. P. (2005) *Biochim. Biophys. Acta* **1745**, 254–264
10. Natochin, M., Gasimov, K. G., and Artemyev, N. O. (2001) *Biochemistry* **40**, 5322–5328
11. Willard, F. S., McCudden, C. R., and Siderovski, D. P. (2006) *Cell. Signal.* **18**, 1226–1234
12. Kimple, R. J., Willard, F. S., and Siderovski, D. P. (2002) *Mol. Interv.* **2**, 88–100
13. Bernard, M. L., Peterson, Y. K., Chung, P., Jourdan, J., and Lanier, S. M. (2001) *J. Biol. Chem.* **276**, 1585–1593
14. Ghosh, M., Peterson, Y. K., Lanier, S. M., and Smrcka, A. V. (2003) *J. Biol. Chem.* **278**, 34747–34750
15. Schaefer, M., Petronczki, M., Dorner, D., Forte, M., and Knoblich, J. A. (2001) *Cell* **107**, 183–194
16. Yu, F., Wang, H., Qian, H., Kaushik, R., Bownes, M., Yang, X., and Chia, W. (2005) *Genes Dev.* **19**, 1341–1353
17. Natochin, M., Lester, B., Peterson, Y. K., Bernard, M. L., Lanier, S. M., and Artemyev, N. O. (2000) *J. Biol. Chem.* **275**, 40981–40985
18. Sato, M., Gettys, T. W., and Lanier, S. M. (2004) *J. Biol. Chem.* **279**, 13375–13382
19. Izumi, Y., Ohta, N., Hisata, K., Raabe, T., and Matsuzaki, F. (2006) *Nat. Cell Biol.* **8**, 586–593
20. Siller, K. H., and Doe, C. Q. (2009) *Nat. Cell Biol.* **11**, 365–374
21. Guo, X., and Gao, S. (2009) *Cell Res.* **19**, 838–848
22. Wiser, O., Qian, X., Ehlers, M., Ja, W. W., Roberts, R. W., Reuveny, E., Jan, Y. N., and Jan, L. Y. (2006) *Neuron* **50**, 561–573
23. Kinoshita-Kawada, M., Oberdick, J., and Xi, Zhu, M. (2004) *Brain Res. Mol. Brain Res.* **132**, 73–86
24. Kimple, R. J., Willard, F. S., Hains, M. D., Jones, M. B., Nweke, G. K., and Siderovski, D. P. (2004) *Biochem. J.* **378**, 801–808
25. Abramow-Newerly, M., Ming, H., and Chidiac, P. (2006) *Cell. Signal.* **18**, 2209–2222
26. Mao, H., Zhao, Q., Daigle, M., Ghahremani, M. H., Chidiac, P., and Albert, P. R. (2004) *J. Biol. Chem.* **279**, 26314–26322
27. Cladman, W., and Chidiac, P. (2002) *Mol. Pharmacol.* **62**, 654–659
28. Berman, D. M., Wilkie, T. M., and Gilman, A. G. (1996) *Cell* **86**, 445–452
29. Watson, N., Linder, M. E., Druey, K. M., Kehrl, J. H., and Blumer, K. J. (1996) *Nature* **383**, 172–175
30. Gruen, J. R., and Weissman, S. M. (2001) *Front. Biosci.* **6**, D960–D972
31. Moulds, J. M. (2001) *Front. Biosci.* **6**, D986–D991
32. Tall, G. G., and Gilman, A. G. (2005) *Proc. Natl. Acad. Sci. U.S.A.* **102**, 16584–16589
33. Thomas, C. J., Tall, G. G., Adhikari, A., and Sprang, S. R. (2008) *J. Biol. Chem.* **283**, 23150–23160
34. Kerr, D. S., Von Dannecker, L. E., Davalos, M., Michaloski, J. S., and Malnic, B. (2008) *Mol. Cell. Neurosci.* **38**, 341–348
35. Natochin, M., Campbell, T. N., Barren, B., Miller, L. C., Hameed, S., Artemyev, N. O., and Braun, J. E. (2005) *J. Biol. Chem.* **280**, 30236–30241
36. Garcia-Marcos, M., Ghosh, P., and Farquhar, M. G. (2009) *Proc. Natl. Acad. Sci. U.S.A.* **106**, 3178–3183
37. Cismowski, M. J., Ma, C., Ribas, C., Xie, X., Spruyt, M., Lizano, J. S., Lanier, S. M., and Duzic, E. (2000) *J. Biol. Chem.* **275**, 23421–23424
38. Strittmatter, S. M., Valenzuela, D., Sudo, Y., Linder, M. E., and Fishman, M. C. (1991) *J. Biol. Chem.* **266**, 22465–22471
39. Lee, M. J., and Dohlman, H. G. (2008) *Curr. Biol.* **18**, 211–215
40. Li, S. S. (2005) *Biochem. J.* **390**, 641–653
41. Williamson, M. P. (1994) *Biochem. J.* **297**, 249–260
42. Garbay, C., Liu, W. Q., Vidal, M., and Roques, B. P. (2000) *Biochem. Pharmacol.* **60**, 1165–1169
43. Gureasko, J., Galush, W. J., Boykevich, S., Sondermann, H., Bar-Sagi, D., Groves, J. T., and Kuriyan, J. (2008) *Nat. Struct. Mol. Biol.* **15**, 452–461
44. Lao, D. H., Chandramouli, S., Yusoff, P., Fong, C. W., Saw, T. Y., Tai, L. P.,

- Yu, C. Y., Leong, H. F., and Guy, G. R. (2006) *J. Biol. Chem.* **281**, 29993–30000
45. Oshiro, T., Koyama, S., Sugiyama, S., Kondo, A., Onodera, Y., Asahara, T., Sabe, H., and Kikuchi, A. (2002) *J. Biol. Chem.* **277**, 38618–38626
46. Higashijima, T., Burnier, J., and Ross, E. M. (1990) *J. Biol. Chem.* **265**, 14176–14186
47. Jordan, J. D., Carey, K. D., Stork, P. J., and Iyengar, R. (1999) *J. Biol. Chem.* **274**, 21507–21510
48. Luo, Y., and Denker, B. M. (1999) *J. Biol. Chem.* **274**, 10685–10688
49. Kopein, D., and Katanaev, V. L. (2009) *Mol. Biol. Cell* **20**, 3865–3877
50. Bourne, H. R. (1997) *Curr. Opin. Cell Biol.* **9**, 134–142
51. Cabrera-Vera, T. M., Vanhauwe, J., Thomas, T. O., Medkova, M., Preininger, A., Mazzoni, M. R., and Hamm, H. E. (2003) *Endocr. Rev.* **24**, 765–781
52. Mahon, M. J., Bonacci, T. M., Divieti, P., and Smrcka, A. V. (2006) *Mol. Endocrinol.* **20**, 136–146